FIBER ALIGNMENT EVALUATION THROUGH X-RAY COMPUTED TOMOGRAPHY

Jennifer M. Sietins[1], Daniel B. Knorr, Jr.[1], Jessica C. Sun[2]
[1] U.S. Army Research Laboratory Aberdeen Proving Ground, MD 21005
[2] Bennett Aerospace, Cary, NC

ABSTRACT

High fiber alignment in composites made from discontinuous fibers is well known to be critical for improved tensile strength in the fiber direction. Advances in laboratory X-ray micro-computed tomography (CT) systems have enabled the three-dimensional visualization of composites at a high enough resolution to quantitatively measure fiber orientations. CT scan settings were optimized for improved image quality and important scanning considerations are discussed. Volume Graphics software was utilized to quantify carbon fiber orientations, and the results were independently validated through optical microscopy. Additionally, results of a sensitivity analysis for various software parameters and thresholding levels will be presented. This paper summarizes the methodology of a new technique for quantifying fiber orientations from high resolution CT scans and potential applications are discussed.

1. INTRODUCTION

It is well known that fiber alignment plays an important role for material properties as the misaligned fibers introduce shear stresses in the softer, polymer matrix and reduce the overall strength. Several techniques have been used to quantify fiber orientations, including different image-based techniques. Optical and scanning electron microscopy have been used for cross-sectional imaging with the shape (circular versus ellipsoidal) of the fibers used to quantify the alignment [1]. Other techniques have included tracking the centroid of the fiber with serial sectioning and confocal laser scanning microscopy [2]. To ensure the accuracy of the spacing between images with serial sectioning methods, some researchers have employed robotic methods to have automated polishing with a specific depth accuracy [3].

More recently, X-ray computed tomography (CT) systems have advanced to be able to obtain high resolution scans within a laboratory setting. This technique has been utilized for the three-dimensional, non-destructive imaging of composites with subsequent analysis of the fiber orientations. Emerson et al. programmed a training algorithm for first automating the fiber segmentation and secondly running a fiber tracking algorithm [4]. Similarly, Czabaj et al. programmed template matching and fiber tracking algorithms, but also converted the segmented fibers into a solid model for finite element analysis [5].

This study utilizes a commercially available software program for orientation analysis, eliminating the need for writing a custom image processing algorithm. Because the specific details of the commercially available algorithm are not openly shared, it is important to study how the analysis parameters influence the results and to independently validate the results, which is the aim of this paper.

2. EXPERIMENTATION

2.1 Sample Preparation

In order to directly compare optical microscopy measurements and orientations measured from the CT scan, a sample with two individual IM7 carbon fibers was made. The 5.2 µm diameter [6] fibers were placed at an angle within a flat mold and dicyclopentadiene (DCPD) resin was added and cured using first generation Grubbs' catalyst.

2.2 X-ray Computed Tomography Scanning Parameter Optimization

There are numerous variables for scanning parameters, including: voltage, current, source-sample distance, sample-detector distance, exposure time, pixel binning, and number of projections. Many of these scanning parameters directly influence the quality of the resulting images. Some of the main considerations for quality scan results are the scan resolution, signal to noise ratio, and the geometric unsharpness. The resolution needs to be adequate relative to the size of the features of interest, which in this case is the diameter of the carbon fiber. It is generally recommended to have at least 5 pixels across a feature of interest for detectability [7]. The signal to noise ratio is influenced by the overall photon count, which is influenced by the source to detector spacing, the scan power, and the exposure time. Additionally, the number of projections influences the noise per the Nyquist theorem.

The geometric unsharpness impacts the edge blurriness and is calculated by the focal spot size times the ratio of the sample to detector distance divided by the source to sample distance. This is illustrated in the schematic of Figure 1. Therefore, it is beneficial to keep the scanning power as low as possible and the detector closer to the sample.

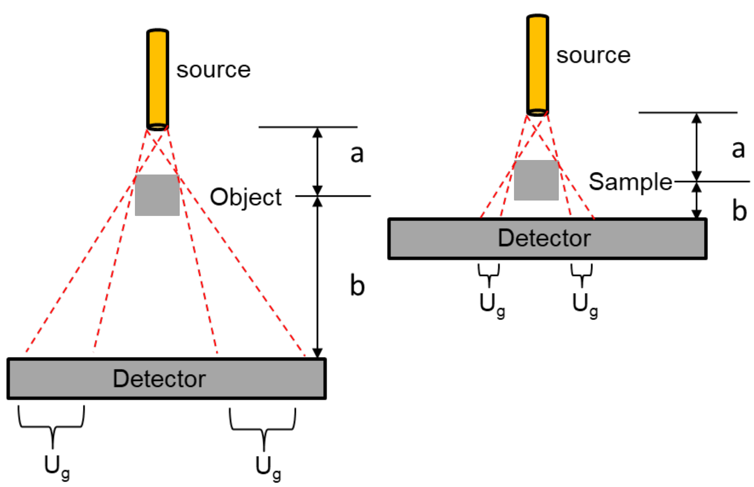

Figure 1. Schematic illustration of the geometric unsharpness, which causes blurriness of edges

The Zeiss Xradia 520 Versa is a unique laboratory-scale CT system in that it incorporates scintillator screens with objective lenses for magnification rather than strictly relying on the source-sample-detector spacings for geometric magnification. This allows the detector to be kept close to the sample, therefore reducing the geometric unsharpness and improving the signal-noise ratio. Figure 2 illustrates the importance of keeping the detector close on a scan of a titanium particle that was approximately 25 μm in diameter. Figure 2A had a large sample-detector spacing of 196 mm and a calculated geometric unsharpness of 4.7 times the focal spot size, whereas Figure 2B had a 15.9 mm sample-detector spacing and a calculated geometric unsharpness of 0.6 times the focal spot size.

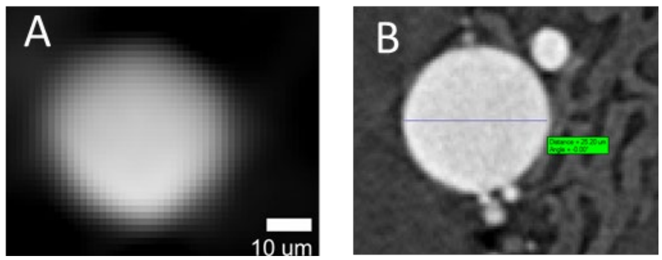

Figure 2. A) Geometric unsharpness of 4.7 times the focal spot size and B) 0.6 times the focal spot size

To keep the geometric unsharpness low and the signal to noise ratio high, the detector was kept close and scans at the three different objective lenses were conducted: 4X, 20X and 40X. This would result in three different scan resolutions and scan volumes with the aim of finding adequate resolution at the largest possible scan volume. The voltage and power were kept low at 50kV, 4W for all of the scans in order to reduce x-ray scattering noise and to keep the focal spot size small.

2.3 Alignment Measurement

Three different methods were used to quantify the fiber orientations for an independent comparison. Volume Graphics software with the composite fiber orientation module, OrientationJ plug-in for ImageJ, and FiberFit methods were each conducted on the same sample. The OrientationJ module utilized a gradient-based tensor method [8] and the FiberFit program used a fast Fourier transformation (FFT) method [9].

2.3.1 Volume Graphics

The composite fiber analysis module was used in Volume Graphics 3.0 to quantify the orientations and export histograms of the results. First, the precise boundary between what is considered to be fiber versus matrix was determined by using the auto-threshold surface determination with the 'reduction of small noise particles' option selected. Then, the region of interest for the analysis was defined as a slightly larger volume (using the dilation function) of the surface determination in order to allow for an adequate number of voxels surrounding the analysis volume so there would not be edge effects. There are several settings within the analysis module that can be adjusted, so it was of interest to perform a sensitivity study on the analysis parameters. First, different analysis modes were explored, including the effect of sample rotation on the orientation results. Additionally, other analysis parameters were adjusted including the scale and integration area size. The scale is used to define the grid point resolution of the analysis and the integration area is used to define distance surrounding each grid point. These parameters were chosen to be 0.5, 0.75, and 1 voxels and 1, 2, and 3 voxels, respectively.

2.3.2 OrientationJ

The OrientationJ plug-in for ImageJ employs a version of the gradient-based tensor method. In this method, a tensor of local gradients within the image are calculated to generate the primary local direction of the gradient. After the CT image stack was loaded, the “Z project” function was used to obtain a single image that accounted for both fibers through the thickness. Then, the Gaussian gradient algorithm was used to quantify the histogram response.

2.3.3 FFT Method

Another method for processing optical data is the fast Fourier transform-based method. Lujan’s group developed this method extensively and produced and validated a program called FiberFit, which can be used to obtain orientation information for two dimensional optical images [9]. The FiberFit program was also compared to the gradient tensor methods mentioned above, and it compared favorably [9]. FiberFit has recently been used to assess orientation of biological samples, including those that contain tissue with fibrillar structures [10].

FiberFit first takes the image and applies a fast Fourier transform algorithm. Then, a band-pass filter is applied to reduce noise. Finally, the data are fit using two variables that describe the mean fiber orientation and fiber dispersion. For our purposes, these two variables are of less significance than the histogram produced by the program, which can be used to obtain relative alignment for simple, two-fiber samples. It should be noted here that performing optical microscopy on carbon fiber reinforced composites with very high loadings is difficult, since this would make the sample opaque and make the analysis meaningless.

3. EXPERIMENTATION

3.1 Scanning Parameter Optimization

Scans were conducted with the 4X, 20X, and 40X objective lenses and representative cross-sectional images are shown in Figure 3. As expected, the 4X objective lens with the 2 µm voxel size (Figure 3A) shows that the resolution was too low relative to the diameter of the fiber. The 20X objective lens with the 0.7497 µm voxel size had adequate resolution. Although the 40X objective lens provided the best resolution with a 0.3763 µm voxel size, the overall scan volume is very limiting with less than a 0.4 mm field of view. Therefore, the 20X 0.7497 µm voxel size scanning resolution was considered the best balance of resolution and field of view and was used for subsequent analysis.

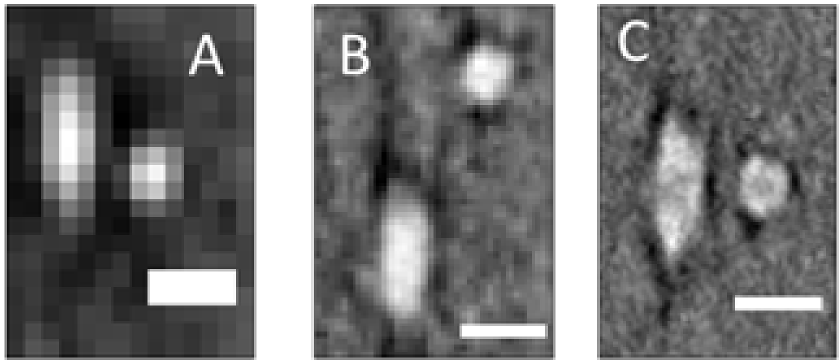

Figure 3. Representative cross-sectional images A) 4X objective lens with a 2 µm voxel size B) 20X objective lens with a 0.7497 µm voxel size C) 40X objective lens with a 0.3763 µm voxel size; all scale bars are 10 µm wide

3.2 Alignment Measurement

3.2.1 Volume Graphics

The various modes within the composite fiber orientation module of Volume Graphics were explored for determining the optimal analysis settings. The space orientation and integration mesh modes did not result in a histogram response which was of interest, so the focus was on using the reference plane mode or the plane projection mode. It was observed that the sample rotation had a major influence on the results when using the reference plane mode as seen in Figure 4. When the two fibers were oriented at approximately 5 and 35 degrees, there were two distinct peaks represented in the histogram response, but when the sample was rotated to approximately +/- 15 degrees, a mirroring effect resulted in the peaks being nearly identical. The projection mode overcame this issue, however, and plots the results on a scale of 0 to 180 degrees rather than 0 to 90, eliminating the mirroring effect or any influence sample rotation may have on the histogram results.

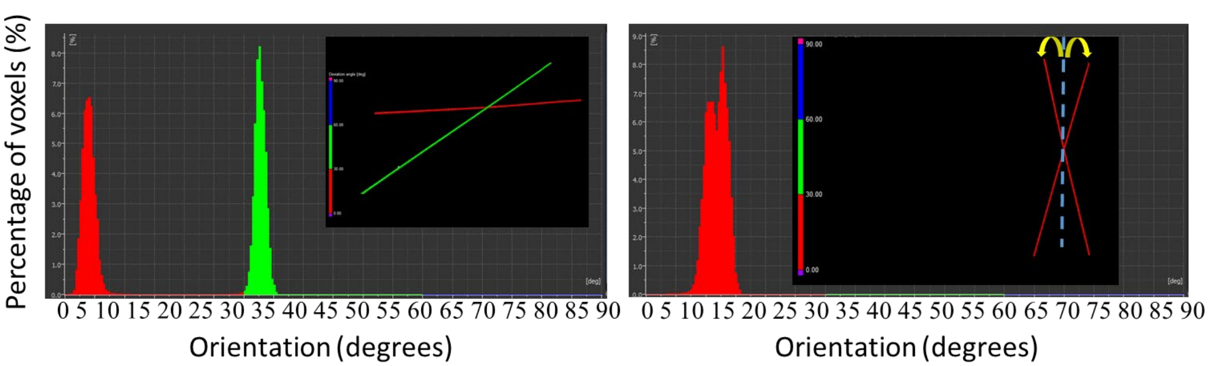

Figure 4. Influence of image rotation on the orientation results when using the reference plane analysis mode: (left) sample rotated to approximately 5 and 35 degrees results in two distinct peaks in the histogram response, (right) sample rotated to approximately +/- 15 degrees resulting in a mirroring effect with a single peak that was clearly erroneous.

Next, the main analysis parameters needed to be optimized when using the plane projection mode. The scale (which defines the number and size of grid points) was adjusted from 0.5, 0.75, and 1 voxels, and the results are shown in Figure 5 for integration areas (the search distance surrounding the grid points) of 1, 2, and 3 voxels. In all cases, the largest scale of 1 resulted in the narrowest width of the histogram. Since a narrow histogram is expected for a sample with only two individual fibers, a scale of one was selected as the scale setting to use for subsequent analysis.

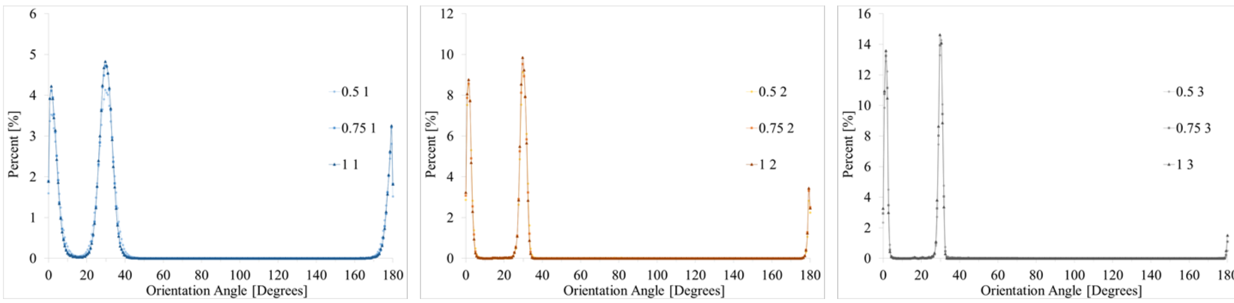

Figure 5. Influence of the scale at input parameters of 0.5, 0.75, and 1 with integration areas of: A) 1, B) 2, and C) 3

The data was also plotted within groupings of the same scale to explore the influence of the integration area, and the results are seen in Figure 6. The integration area of 3 had the narrowest width and highest peak. Therefore, the results of the analysis with the settings of a scale of 1 and integration area of 3 were directly compared with the optical microscopy results.

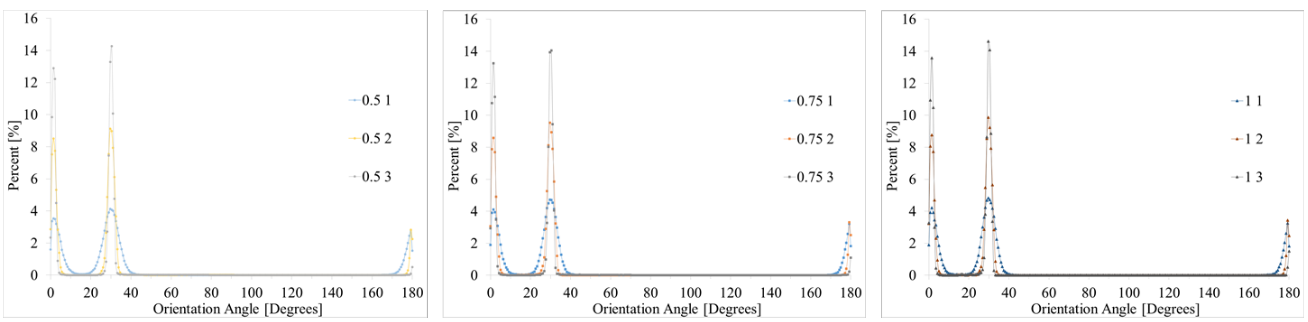

Figure 6. Influence of integration area size with scales of: A) 0.5, B) 0.75, and C) 1

3.2.2 OrientationJ

The histogram response from OrientationJ is shown in Figure 7, with peaks at approximately 0 and 30 degrees.

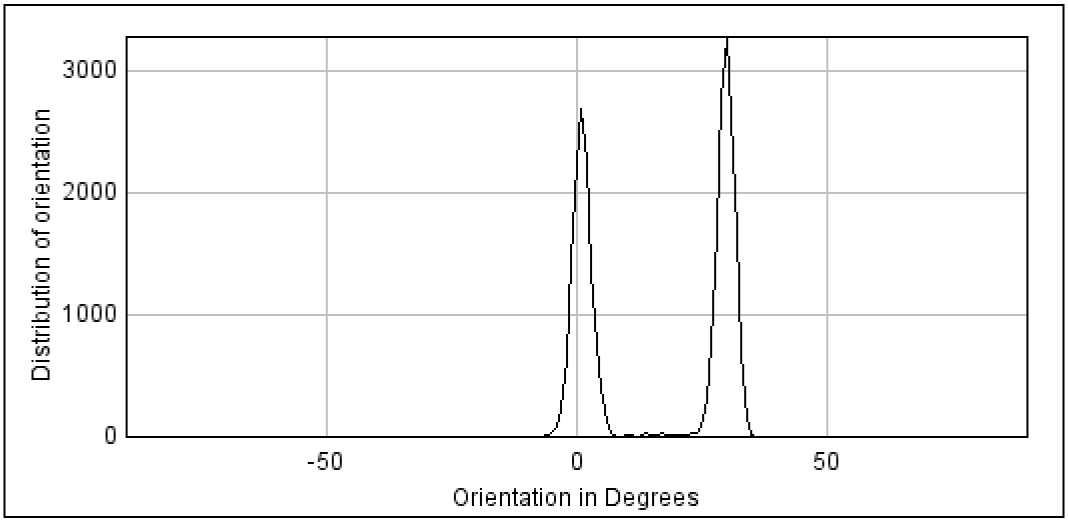

Figure 7. Histogram response of the Gaussian gradient analysis method within OrientationJ

The raw data was exported and plotted on the same graph as the Volume Graphics data with the analysis settings previously described. The results are shown in Figure 8, which shows an excellent agreement between the Volume Graphics results and OrientationJ results.

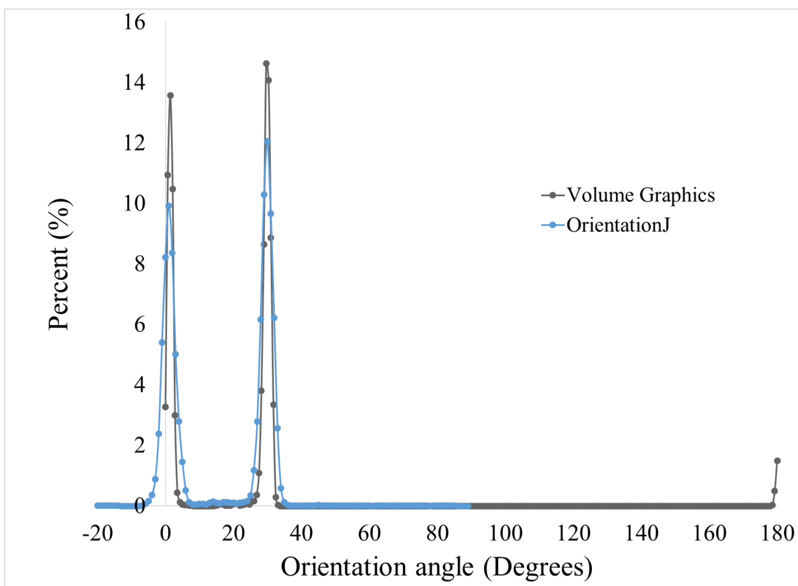

Figure 8. Direct comparison of Volume Graphics and OrientationJ results show excellent agreement

3.2.3 FiberFit

The FiberFit program was used to assess the orientation of the same sample used in the previous subsection. These results are provided in Figure 9, which shows the original microscope image, the resulting FFT image and histograms of results. As shown, the results provide data that are essentially identical to those above, where one fiber is assigned to a zero degree alignment, and the other is aligned at 30 degrees. While this method provides confirmation of the above and useful guidance, the histogram of the data unfortunately cannot be exported from the program, which limits the utility of FiberFit.

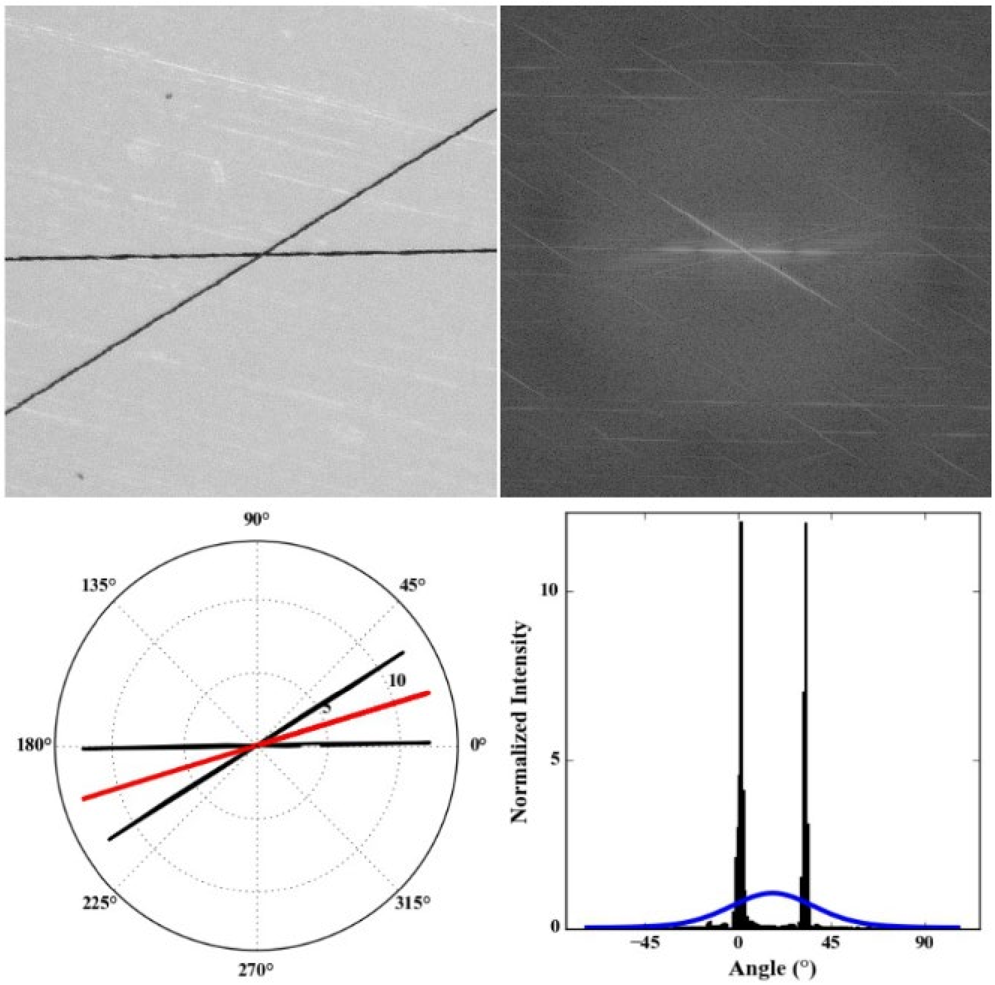

Figure 9. FiberFit results: (top left) original 5x microscope image of carbon fiber/polydicyclopentadiene sample, (top right) band-pass filtered fast Fourier transform results obtained from the microscope image, (lower left) 360 degree plot showing the distribution of the fiber orientations, (lower right) histogram with the same information. The red line and blue line represent the averages, which are meaningless in this case.

4. CONCLUSIONS

In summary, three different analysis methods were utilized on the CT dataset which showed excellent agreement between one another. The scanning resolution of 0.7497 µm was determined to provide adequate resolution with the largest field of view possible. This was achieved by keeping the detector as close as possible to the sample, reducing the geometric unsharpness and improving the signal to noise ratio and then applying the 20X objective lens for magnification. The Volume Graphics orientation analysis settings were determined to be a scale of 1 and an integration area of 3 to provide a narrower peak at a given fiber orientation, which would be expected for two individual fibers.

Although the Volume Graphics orientation analysis technique shows a lot of promise, there are some shortcomings. In particular, the fact the histogram response is a function of the analysis settings that are selected, the analysis should primarily be used for approximations or relative comparisons of samples that were scanned and analyzed under the same conditions. This may be beneficial for process optimization purposes when scanning several samples at various processing controls, but scanned and analyzed with identical settings.

This research was developed with funding from the Defense Advanced Research Projects Agency (DARPA). The views, opinions and/or findings expressed are those of the author and should not be interpreted as representing the official views or policies of the Department of Defense or the U.S. Government.

5. REFERENCES

1. Creighton, C. J., Sutcliffe, M. P. F., Clyne, T. W. A multiple field image analysis procedure for characterization of fibre alignment in composites. *Composites Part A: Applied Science and Manufacturing* 32 (2001) 221-229.

2. Eberhardt, C. Clarke, A. Fibre-orientation measurements in short-glass-fibre composites. Part I: automated, high-angular-resolution measurement by confocal microscopy *Composites Science and Technology* 61 (2001) 1389-1400.

3. Bricker, S. Simmons, J. P., Przybyla, C., Hardie, R. C. Anomaly detection of microstructural defects in continuous fiber reinforced composites. Proceedings of the SPIE/IS&T Electronic Imaging Volume 9401, Computational Imagining XIII (2015).

4. Emerson et al. Individual fibre segmentation from 3D X-ray computed tomography for characterizing the fibre orientation in unidirectional materials *Composites Part A: Applied Science and Manufacturing* 97 (2017) 83-92.

5. Czabaj, M. W., Riccio, M. L., Whitacre, W. W. Numerical reconstruction of graphite/epoxy composite microstructure based on sub-micron resolution X-ray computed tomography *Composites Science and Technology* 105 (2014) 174-182.

6. HexTow® IM7 Product Datasheet accessed at https://www.hexcel.com/user_area/content_media/raw/IM7_HexTow_DataSheet.pdf on January, 10 2019.

7. Patterson, B., Escobedo-Diaz, J., Dennis-Koller, D., Cerreta, E. Dimensional quantification of embedded voids or objects in three dimensions using X-ray tomography. *Microscopy and Microanalysis* 18 (2012) 390-398.

8. Bigun, J., Bigun, T., Nilsson, K. Recognition by symmetry derivatives and the generalized structure tensor, *IEEE Transactions on Pattern Analysis and Machine Intelligence* 26 (2004) 1590-1605.

9. Morill et al., A validated software application to measure fiber organization in soft tissue. *Biomechanics and Modeling in Mechanobiology* 15 (2016) 1467-1478.

10. Frahs et al., Extracellular Matrix Expression and Production in Fibroblast-Collagen Gels: Towards an In Vitro Model for Ligament Would Healing, *Annals of Biomedical Engineering*, Nov. 2018, v. 46, issue 11, pp. 1882-1895.